



Inter-comparison of high-resolution satellite precipitation products over India during the summer monsoon season

Tirumani Siva Saikrishna¹ · Dandi Appala Ramu² · Krishna Kishore Osuri¹

Received: 1 March 2021 / Accepted: 25 August 2021 / Published online: 27 September 2021
© The Author(s), under exclusive licence to Springer-Verlag GmbH Austria, part of Springer Nature 2021

Abstract

Water management and risk hazard analysis demand high-resolution (spatially and temporally) rainfall. The present study evaluates recently developed high-resolution satellite precipitation products such as global precipitation measurement (GPM), Indian National Satellite System (INSAT) multi-spectral rainfall algorithm (IMR), INSAT hydrometer estimation method (HEM), and Tropical Rainfall Measuring Mission (TRMM) for Indian summer monsoon during 2014–2019 against India Meteorological Department (IMD) gridded product. Overall, the GPM is remarkably captured spatial distribution of seasonal mean rainfall over India and monsoon dominated zones (i.e. western ghats, eastern and central India). Most satellite products overestimated the seasonal rainfall except the GPM (6.8 mm day^{-1}), closely matched with IMD rainfall (6.5 mm day^{-1}). GPM is skillful for different rainfall categories such as light ($< 7.5 \text{ mm day}^{-1}$), moderate ($7.6\text{--}64.4 \text{ mm day}^{-1}$), and heavy ($> 64.5 \text{ mm day}^{-1}$) on monthly and seasonal scales over all homogeneous regions. In case of INSAT products, the HEM showed improved results than the IMR for all the rainfall thresholds in all homogeneous regions. Similarly, the evaluation of satellite products for (deficit-year (2015) and normal-year (2016) reveals that GPM is superior to both the INSAT and TRMM rainfall products. The analysis of daily rainfall extremes indicates that GPM rainfall could replicate the same for the lowest, normal and highest rain categories compared with the others. The performance of INSAT rainfall can be improved by merging with rain-gauge data, suitable bias corrections, and providing hydrometeors information.

1 Introduction

Precipitation is an essential meteorological parameter not only in the view of energy generation, and water management but also in the view of socio-economic impact over India (Gadgil and Kumar 2006). During the summer monsoon season (June–September, hereafter JJAS), the Indian landmass receives a maximum amount of rainfall ($\sim 80\%$ of the annual total rainfall) with significant spatio-temporal variability (Krishnamurthy and Shukla 2007, Turner and Annamalai 2012, Guhathakurta and Rajeevan 2008). The variability of Indian summer monsoon rainfall (IMSR) at the

regional scale is necessary for the hydrological cycle (Liu et al. 2017; Larson and Peck 1974; Jiang et al. 2012) and demands a good observational network. The conventional rain gauges are limited and irregularly spaced with irregular maintenance over India. Though radars are providing high-resolution information, it has failed to cover a large area (confined to a few hundred km (250–500 km), Tapiador et al. 2012). The satellite measurements overcome this problem and providing rainfall data continuously as a substitution to the *in situ* data at reasonable temporal and spatial resolution (Huffman et al. 2015). Accurate and reliable rainfall at possible high spatio-temporal resolution boosts hydrological studies and numerical weather prediction (NWP) at various temporal scales (Krishnamurthy and Kinter 2003).

Worldwide, many operational centres develop and improve satellite-derived rainfall products at various temporal and spatial resolutions (Sun et al. 2018). The Tropical Rainfall Measuring Mission (TRMM) is the one that has a significant contribution to the scientific community in providing rainfall data by combining both Infrared and microwave information (Kummerow et al. 1998). The improved TRMM product uses rain-gauge observations (Huffman

Communicated by xinxin xie.

✉ Krishna Kishore Osuri
osurikishore@gmail.com

¹ Department of Earth and Atmospheric Sciences, National Institute of Technology Rourkela, Rourkela, Odisha 769 008, India

² Indian Institute of Tropical Meteorology, Pune, Maharashtra 411 008, India

et al. 2007) that has been widely accepted and used by the research, scientific, and real-time application purposes (Dinku et al. 2008; Nair et al. 2009; Rahman et al. 2009; Mitra et al. 2009; Houze 2012; Mitra et al. 2013; Uma et al. 2013; Gairola et al. 2014; Derin and Yilmaz 2014; Mei et al. 2014; Prakash et al. 2015b, c, a). This rainfall estimation is a well-accepted data set and widely used in monsoon studies (Prakash et al. 2015a, b) and tropical cyclones (Ankur et al. 2020, Osuri et al. 2020), etc.

In recent years, Huffman et al. (2015) developed Integrated Multi-Satellite Retrievals for Global Precipitation Measurement (IMERG/GPM, hereafter GPM) by merging the precipitation information from the satellite network. It is known that GPM is the successor of the TRMM satellite with significant improvement both in spatial ($0.1^\circ \times 0.1^\circ$) and temporal (30 min) resolution. Due to its high spatio-temporal resolution, recent studies have widely used the GPM in the field of weather forecasting (Bushair et al. 2019), validation of model outputs (Mukhopadhyay et al. 2019), hydrological cycle management (Lakshmi Kumar et al. 2014; Singh et al. 2018) and decision-making applications (Reddy et al. 2019; Thakur et al. 2020). Recently, the Indian Satellite Research Organization (ISRO) has started developing rainfall products such as Indian National Satellite System (INSAT) Multispectral Rainfall Algorithm (hereafter IMR), and INSAT Hydrometer Estimation Method (hereafter HEM) using INSAT-3D information over land and ocean (Kumar and Varma 2017). Mitra et al. (2018) demonstrated that the IMR product is better for light to moderate rainfall, while HEM is good for heavy rainfall over India.

IMD has been preparing the gridded rainfall dataset based on a variable network of rain gauge stations. Rajeevan et al. (2006) developed the gridded daily rainfall at a spatial resolution of $1^\circ \times 1^\circ$. With the increase in the rain gauge network, the rainfall dataset has been updated from time to time to $0.5^\circ \times 0.5^\circ$ (Rajeevan et al. (2009), and then recently to $0.25^\circ \times 0.25^\circ$ resolution (Pai et al. 2014). The dataset has been widely used to estimate/validate remote sensing, analysis/re-analysis, and modelled rainfall products (Prakash et al. 2015b, c, a; Uma et al. 2013; Rajeevan et al. 2006). This dataset has also played a vital role in understanding the hydrological cycle and climate variability of a region (Pai et al. 2015; Lakshmi Kumar et al. 2014). IMD data showed a correlation of more than 0.80 against the global dataset (Pai et al. 2014). The performances of satellite rainfall products compared with the Indian Meteorological Department (hereafter IMD) rainfall are examined over central India (Prakash et al. 2015b, c, a; Kumar et al. 2019; Thakur et al. 2020).

The objective of the study is to assess the accuracy and reliability of recently developed satellite (GPM and INSAT-3D) rainfall products against IMD gridded rainfall (Pai et al. 2014, 2015) as well as established TRMM rainfall. Besides, the study also addresses the performance of the satellite

products for (1) different monsoon homogeneous regions of India at different temporal (daily and inter-seasonal) scales and (2) extreme (deficit and normal) monsoon years during 2014–2019. This study identifies the reliability of satellite products for hydro-meteorological applications and validation of high-resolution models over the Indian region.

2 Data

IMD collects rainfall information from the dense network of rain gauge stations (about 6955) maintained not only by IMD but also by academic and research organisations of India. Each rain gauge data undergoes two types of tests: the verification of station location and the second one is the quality control test of rainfall. During quality control, check for the extreme value, duplicate station, typing, and coding errors, missing data, etc. The quality controlled data are interpolated to the regular grids using Shepard interpolation method (Shepard et al. 1968) to prepare gridded product (Rajeevan et al. 2006, 2009; Pai et al. 2014, 2014). The dataset mainly covers Indian landmass (6°N – 35°N and 66°E – 95°E). Thus, the IMD dataset has been chosen as a reference to evaluate the satellite rainfall products.

The GPM version 7 rainfall data was jointly developed by the National Aeronautics and Space Administration (NASA) and the Japan Aerospace and Exploration Agency (JAXA) for global converge of 60°S – 60°N at $0.1^\circ \times 0.1^\circ$ spatial resolution and half-hourly temporal resolution and launched in 2014. GPM is a merged product of passive microwave (PMV) and Infrared (IR) sensor estimators. IMERG data are available as early (IMERG-E), late (IMERG-L) and final (IMERG-F) products after 4 hourly, 18 hourly, and 3 months from the observation time, respectively (Huffman et al. 2020). For the present study using a half-hourly IMERG-F product. The daily rainfall product of TRMM Multi-satellite Precipitation Analysis (TMPA-3B42, Huffman et al. 2007) is estimated from the Thermal Infrared (TIR) and Microwave sensors information (given in Table 1). TRMM is available in 3 hourly, daily, and monthly manner with an interval of $0.25^\circ \times 0.25^\circ$ spatial resolution with a spatial coverage of 50°S – 50°N and 0° – 360° E.

The Indigenous INSAT-3D, from the INSAT series of satellites, was launched in July 2013 by ISRO. The HEM and IMR rainfall products have been preparing using different algorithms at a spatial resolution of $\sim 0.1^\circ \times 0.1^\circ$ in different time intervals (half an hour, daily, weekly and monthly) and available at <https://www.mosdac.gov.in>. The IMR uses TIR and water vapour (WV) sensors to classify the cloud categories, such as convective, deep convective, low-level clouds, and cirrus clouds (Roca et al. 2002). The IMR algorithm is carried out with two-step procedure with a spatial coverage of 40°S – 40°N and 30°E – 120°E . In the initial

Table 1 Temporal and spatial resolution of satellite rainfall estimation products

S.no	Satellite precipitation product	Channel used	Spatial resolution (degrees)	Temporal resolution (minutes)	Spatial coverage (degrees)	Data availability (years)
1	Hydro estimator	TIR and NWP model	0.1°×0.1°	30	81°S – 81°N and 3°–163°E	2014 – present
2	INSAT multi-spectral rainfall algorithm (IMR)	TIR and WV	0.1°×0.1°	30	30°E –120°E and 40°S – 40°N	2014 – present
3	Tropical rainfall measurement mission (TRMM)	IR and MW	0.25°×0.25°	180	50° S–50° N and 0°–360° E	1997 – 2019
4	Integrated multi-satellite retrieval for global precipitation measurement (IMERG)	IR and MW	0.1°×0.1°	30	60° S – 60° N and 0–360° E	2014 – present

step, the rain/no rain areas are identified based on IR-based Cloud Top Brightness Temperature (CTBT) and optimizes rain clouds' nature and location (Ba and Gruber 2011). In the second step, a relationship is established between TIR and Precipitation Radar (PR) observation, called the power law regression equation.

$$R = 16.6614 \times \exp [-(CTBT) - 204.57]/16.52688],$$

where R is the rain rate (in mm h^{-1}), and BT is the cloud top brightness temperature of the TIR channel (in K). The major source of error in this scheme could be the incorporating cirrus clouds that produce ice crystals that evaporate before reaching the ground (Barret and Martin 1981).

HEM is an operational product with a spatial coverage of 81°S–81°N and 3°E–163°E. The HEM algorithm uses TIR information and numerical forecasts at high spatial and temporal resolutions. The algorithm is improved by several corrections such as (1) warm rain correction, (2) orography correction, and (3) dry Atmospheric correction using relative humidity data from NWP model output (Kumar and Varma 2017). The detailed information on satellite products is given in Table 1.

3 Methods

The spatial scales of satellite products are different; hence they are interpolated to the IMD rainfall grids (~25 km) using bi-linear interpolation for homogeneous comparison. The ocean/sea region is masked in all the satellite products. Various traditional statistical metrics (bias, correlation coefficient (CC), and root-mean-square error (RMSE)) are used, along with skill metrics for different rainfall categories. A 2×2 contingency table (Table 2) is constructed for the number of hits (occurrence in both satellite and observed),

Table 2 Contingency table for satellite and observation data

Satellite	Observation	
	Rain	No rain
Rain	Hit	False alarm
No rain	Miss	Correct negative
Total	Hit + miss + false alarm + correct negative	

misses (occurrence in observation but no occurrence in satellite), false alarms (occurrence in satellite but no occurrence in observation) and correct negative (no occurrence in both). Based on these metrics, accuracy (ACC), probability of detection (POD), false alarm ratio (FAR), and equitable threat score (ETS) are estimated as follows:

$$ACC = \text{hits} + \text{correct negative} / \text{total}$$

$$POD = \text{hits} / \text{hits} + \text{misses}$$

$$FAR = \text{false alarm} / \text{hits} + \text{false alarms}$$

$$ETS = \text{hits} - \text{hits random} / \text{hits} + \text{misses} + \text{false alarms}$$

$$\text{Hits random} = (\text{hits} + \text{misses}) \times (\text{hits} + \text{false alarms}) / N.$$

The POD represents the correctly detected events of a particular rainfall threshold and ranges from 0 to 1, 0 means no skill and 1 is a perfect score. FAR describes the fraction of rainfall detected by satellite but not present in observation, ranging from 0 to 1, 0 indicates a perfect score. ETS is the fraction of both observed and satellite captured events (captured correctly). It is sensitive to hits and ranges from -1/3 to 1, 0 indicates no skill, and 1 is a perfect score.

The performance of satellite rainfall products is also verified for different categorical rainfall activities over India. In this analysis, IMD defined rainfall categories (based on seasonal rainfall and their inter-annual variations during the summer monsoon) are used. According to IMD criteria, the rainfall thresholds considered in the study are light ($< 7.6 \text{ mm day}^{-1}$), moderate ($7.6 - 64.4 \text{ mm day}^{-1}$), and heavy ($> 64.5 \text{ mm day}^{-1}$) rainfall (Mitra et al. 2018). Note

that the heavy rainfall category includes heavy, very heavy, and extremely heavy rainfall values.

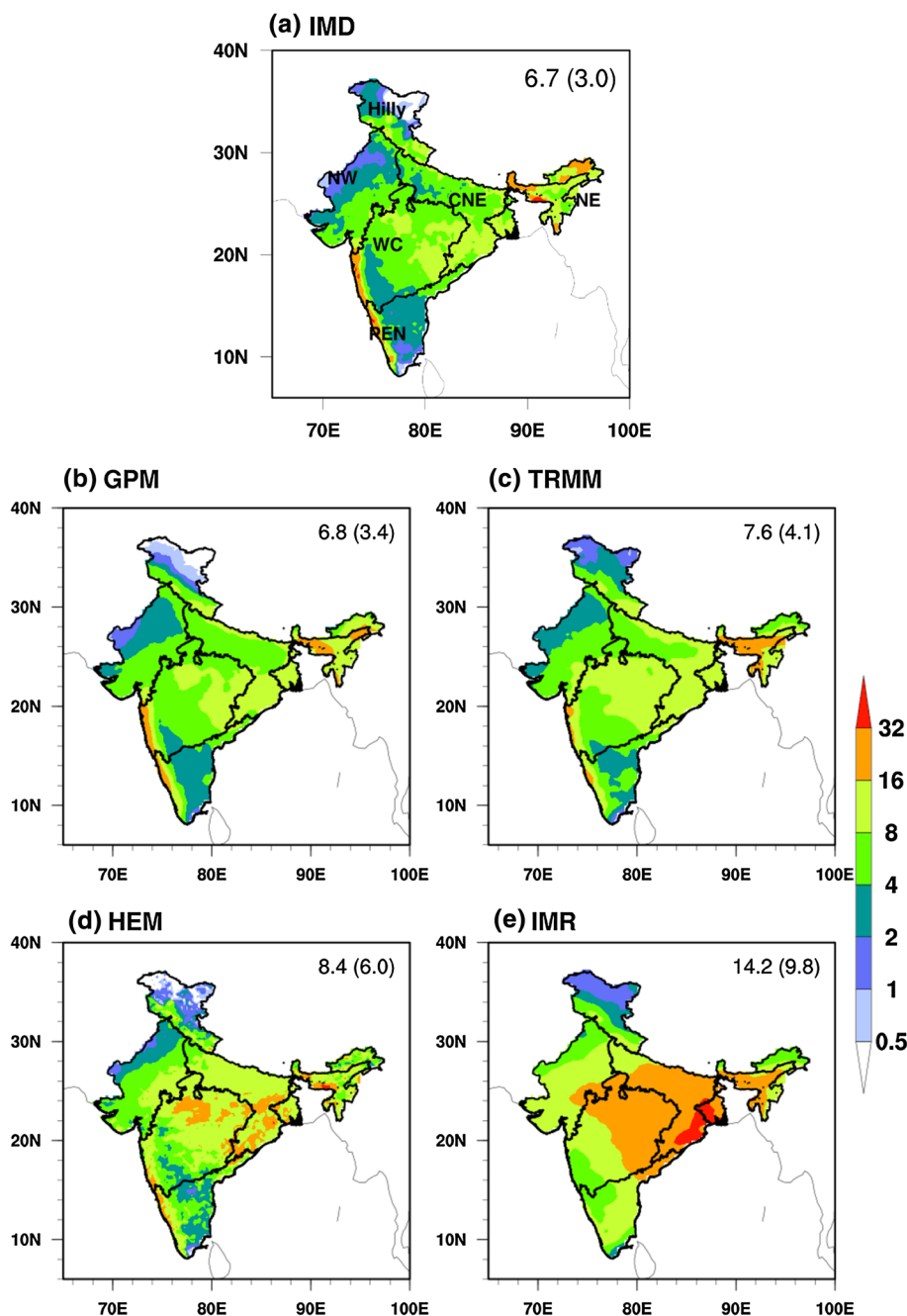
4 Results and discussion

4.1 Spatial and temporal distribution of seasonal rainfall

The spatial and temporal distribution of seasonal rainfall from different satellite products is evaluated against IMD

rainfall over India from 2014 to 2019 and presented in Fig. 1a–e. The observational (IMD) rain revealed, during the season, the maximum rainfall ($> 16 \text{ mm day}^{-1}$) received along the west coast of India and some parts of the north-eastern parts of India. A minimum rainfall ($< 4 \text{ mm day}^{-1}$) received in the north, northwest, and south peninsular regions (Fig. 1a). Around $4\text{--}16 \text{ mm day}^{-1}$ rainfall is received over central India and along the foothills of the Himalayas, which can be attributed to the movement of the monsoon trough (Fig. 1a). There is a strong gradient in JJAS rainfall from the southeast (more rainfall) to northwest (less rain) is

Fig. 1 Spatial distribution of summer monsoon rainfall using **a** IMD, **b** GPM, **c** TRMM, **d** HEM, and **e** IMR over India during 2014–2019. Numbers in the top-right corner of each subplot indicate all-India seasonal mean rainfall and standard deviation. There are six monsoon homogeneous regions such as Hilly, North West (NE), West Central (WC), Central North East (CNE), North East (NE), and Peninsular India (PEN) are represented in the subplot (a)



observed in the IMD observations (Fig. 1a). The boundaries shown in Fig. 1a are representing the six different monsoon homogeneous regions, namely Hilly, North West (NE), West Central (WC), Central North East (CNE), North East (NE), and Peninsular India (PEN).

The GPM and HEM satellite products have reasonably captured the spatial pattern of seasonal rainfall over India as in the observation (Fig. 1b, d). However, a slight overestimation in HEM rainfall is noticed (Fig. 1d) and could be attributed to the HEM product considering numerical forecasts to combine TIR and WV channels information (Singh et al. 2018). Another reason could be the lack of appropriate hydrometeor information in this product. The orographic rainfall along the west coast, northeast and foothills of the Himalayas were captured in GPM ($16\text{--}32\text{ mm day}^{-1}$), while scattered rainfall of a similar amount is noticed in HEM.

On the other hand, the TRMM and IMR products are unable to capture orographic rainfall, particularly along the west coast of India (Fig. 1c, e). Previous studies have also highlighted the difficulty in estimating precipitation over complex topography/orography regions and is attributed to the TRMM rainfall algorithms (Dinku et al. 2008; Derin and Yilmaz 2014). Unlike other products, the IMR overestimates rainfall in the monsoon-core region (central parts) of India by $10\text{--}12\text{ mm day}^{-1}$ as compared to the IMD rainfall. IMR rainfall estimation scheme depends mainly on the CTBT temperature. TIR and WV sensors are getting information from the rainfall producing CTBT and CTBT of cirrus (high level) clouds. Since the cirrus clouds are wispy and contain ice crystals will enhance CTBT temperature. These clouds are produced ice crystals that evaporate before landing on the ground. The algorithm which is using only CTBT for detecting rainfall areas without analysing the cloud system results, either overestimation or underestimation of rainfall over a region (Vicente et al 1998). Therefore, the algorithm is showing more rainfall estimation. All the products exhibited the southeast to northwest rainfall gradient during the season.

The probability density function (PDF) of bias (obtained as satellite minus IMD rainfall), RMSE, and CC of satellite products against IMD rainfall are shown in Fig. 2a–c. It reveals that the GPM rainfall shows less bias (close to zero at 75% frequency), less RMSE (7 mm day^{-1} at 50% frequency), and higher correlations (0.37 at 20% frequency) for all India rainfall. The TRMM and HEM follow the GPM rainfall in capturing all India rainfall. It is to be noted that the IMR exhibited a broader PDF for bias ($10\text{--}15\text{ mm day}^{-1}$ at 15%), higher RMSE ($10\text{--}30\text{ mm day}^{-1}$ at 15%), and less CC (0.21 at 25% frequency). GPM has captured the all-India seasonal rainfall (6.8 mm day^{-1}) and its inter-annual variability (standard deviation, 3.1 mm day^{-1}) and close to that of the IMD rainfall (6.7 mm day^{-1} and 3.0 mm day^{-1} , respectively) (Fig. 1a–e). While the seasonal

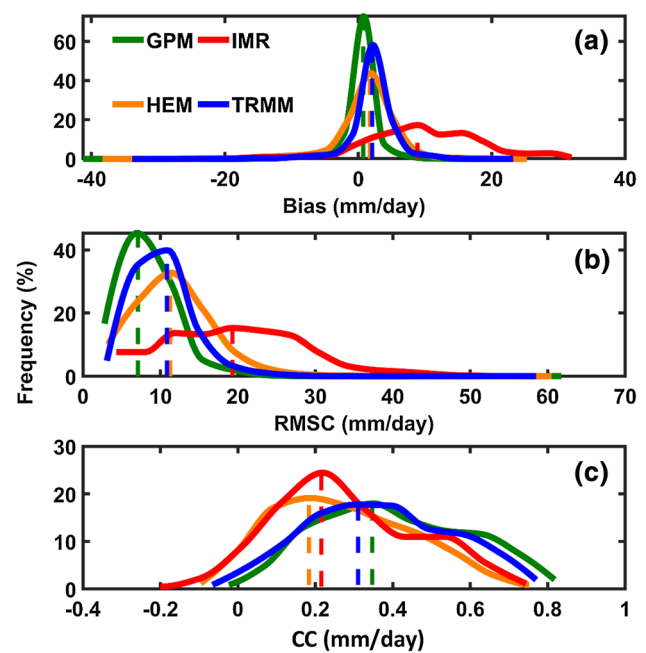


Fig. 2 The probability functions of seasonal mean **a** bias (obtained as satellite minus IMD), **b** RMSE and **c** CC for GPM (green), TRMM (blue), HEM (orange), and IMR (red). These error statistics are calculated against IMD rainfall

all-India rainfall is overestimated in TRMM (7.6 mm day^{-1}), HEM (8.4 mm day^{-1}), and IMR (14.2 mm day^{-1}) products. More substantial inter-annual variability of these products indicates that all these satellite products could identify extreme rainfall in India. The mean error statistics of satellite rainfall are computed against IMD along with 99% confidence intervals (Table 3). Among four satellite products, GPM shows less bias (0.21 ± 0.2) mm day^{-1} , RMSE (7.4 ± 0.36) mm day^{-1} , and higher CC (0.7 ± 0.01). The TRMM rainfall also exhibits fewer errors; RMSE ranges $9.1 \pm 0.55\text{ mm day}^{-1}$, and CC ranges 0.56 ± 0.11 . However, TRMM and HEM rainfall bias is slightly higher ($> 1.5\text{ mm day}^{-1}$). On the other hand, the IMR rainfall has exhibited noticeably higher errors than the other products.

Figure 3 illustrates the PDF (%) of categorical (light, moderate, and heavy) rainfall on a monthly scale from four satellite products. The frequency of light rainfall is slightly higher in GPM throughout the JJAS months (Fig. 3a). The HEM is consistently better than the others for light rain in all the months, exhibiting a similar frequency as that of observation (Fig. 3a). The TRMM is better in June and September (onset and withdrawal months), while it is underestimated in July and August (active) months (Fig. 3a) for all rainfall categories. The IMR frequency is consistently less in all the months (Fig. 3a). In the case of moderate rainfall category, GPM, HEM lacks the frequency of occurrences in all the months, while the TRMM

Table 3 Statistical errors of Indian summer monsoon rainfall are given along with 99% significance

Satellite precipitation product	Bias (99% confidence)	RMSE (99% confidence)	CC (99% confidence)
Integrated multi-satellite retrieval for global precipitation measurement (IMERG)	0.25 (0.2)	7.2 (0.37)	0.73 (0.01)
Tropical rainfall measurement mission (TRMM)	2.2 (0.43)	9.3 (0.55)	0.59 (0.01)
Hydro estimator	1.3 (0.53)	13.0 (0.86)	0.48 (0.02)
INSAT multi-spectral rainfall algorithm (IMR)	10.1 (1.13)	21.2 (1.68)	0.33 (0.02)

99% confidence interval is shown in the parenthesis

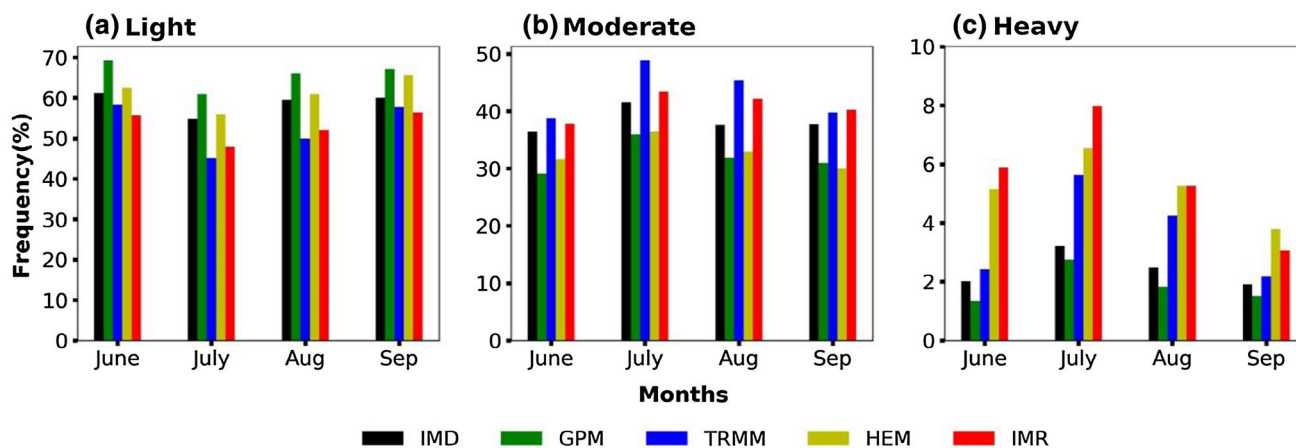


Fig. 3 Month-wise probability density function (%) of all-India mean seasonal rainfall from IMD, GPM, TRMM, HEM, and IMR for **a** light, **b** moderate and **c** heavy rainfall categories

is relatively better in capturing the moderate rainfall when compared with IMD rainfall (Fig. 3b). The heavy rainfall category is less evident in IMD when compared to light and moderate rainfall (Fig. 3c). The GPM could show a similar frequency of heavy rainfall episodes in all the months (Fig. 3c). The heavy rainfall category in the sub-season is overestimated by TRMM and INSAT-3D rainfall products (HEM and IMR). Among the products, the TRMM shows consistent behavior for heavy rainfall, particularly in June and September with overestimation in July and August months. These results are consistent with the previous study by Mitra et al. (2018). It is worthy to note that the TRMM performance is better in the onset (June) and withdrawal (September) months than the active monsoon months (July and August) for all rainfall categories.

The contingency statistics for categorical rainfall are presented in Fig. 4. Inter-comparison of the products indicates that the GPM, TRMM, HEM and IMR exhibited higher POD with relatively smaller FAR and high ETS in identifying the light rainfall (Fig. 4a). The light rainfall in the monsoon season is comparatively well detected in

GPM (~70%), followed by TRMM (60%), HEM (50%), and IMR (50%), respectively. The GPM is more skilful about 0.35 than the other rainfall products whose ETS is less than 0.25 for light rainfall (Fig. 4a). In the case of moderate rainfall, the data products exhibit reduced skill scores in terms of POD and ETS. Though the detection of moderate rainfall in GPM is less (45%), the FAR is minimum among all the products. The TRMM exhibits a higher detection rate of 55% with slightly higher FAR (~60%). Though the HEM and IMR products are relatively better in detecting moderate rainfall (48–50%), the FAR is also higher (>60%). However, the ETS is more or less the same for GPM, TRMM and HEM, while it is much higher (~0.25) for IMR (Fig. 4b). The higher ETS skill in the case of IMR for moderate rainfall could be attributed to its overestimation. The heavy rainfall is well detected in TRMM and HEM products at 30–35% (Fig. 4c). The GPM is also relatively better for heavy rainfall by ~22%. While the IMR is relatively poor for detecting heavy rainfall episodes (Fig. 4c). Considering the FAR, all the products show 90% of false signals for heavy rainfall activity during monsoon season.

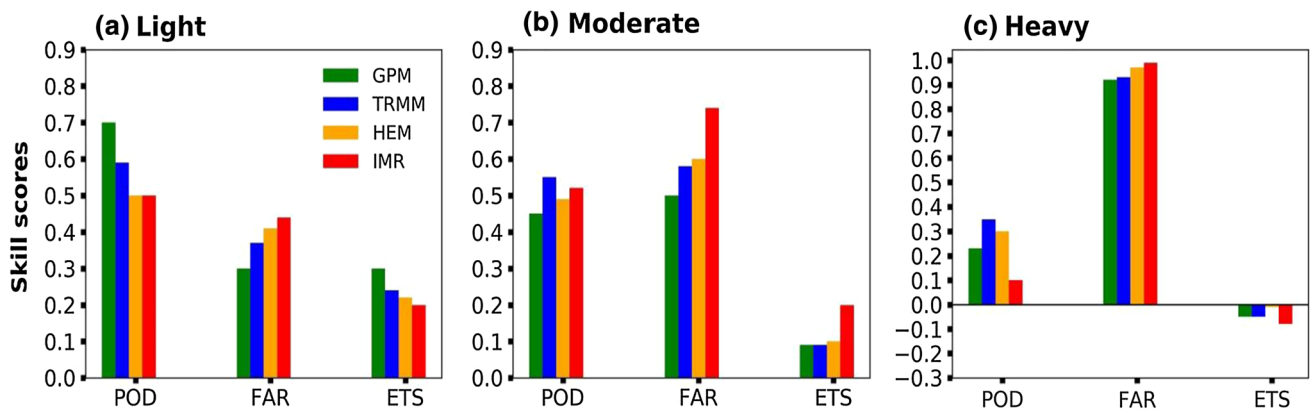


Fig. 4 Skill scores (POD, FAR, and ETS) of all-India mean seasonal rainfall from IMD, GPM, TRMM, HEM, and IMR for **a** light, **b** moderate and **c** heavy rainfall categories

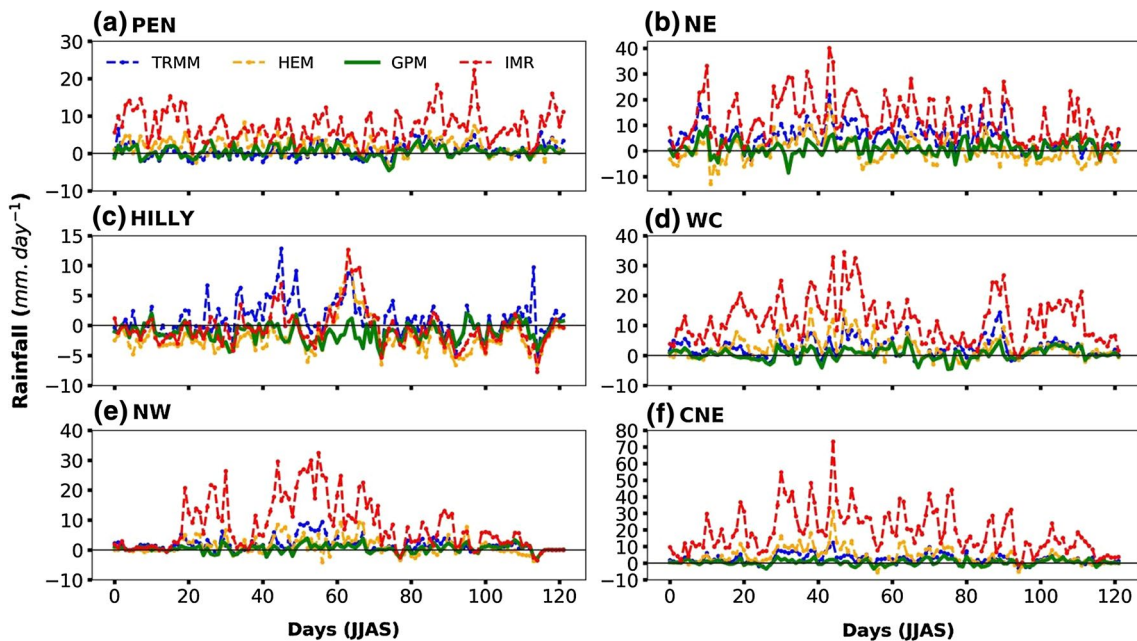


Fig. 5 Average rainfall Errors at daily scale for different monsoon homogeneous regions **a** Peninsular (PEN), **b** Northeast (NE), **c** Hilly, **d** West Central (WC), **e** North West (NW), and **f** Central Northeast

(CNE) from GPM (green), TRMM (blue), HEM (orange) and IMR (red). The error is calculated against IMD rainfall

4.2 Evaluation over monsoon homogeneous regions of India

In addition, the study analyses the performance of satellite products over the above shown six monsoon homogeneous regions (Fig. 1a). The rainfall exhibits high variability in spatial and temporal scales. For example, complex topography such as Western Ghats, Eastern Ghats and the

Himalayas in India plays a crucial role in rainfall intensity and distribution, while the southern peninsular region receives less rainfall (Gadgil 1977). The classification of homogeneous regions is based on similar rainfall characteristics and regional/global teleconnections with monsoon rainfall and is adopted from Parthasarathy et al. (1995). The temporal variation of mean monsoon rainfall for IMD (black), GPM (green), TRMM (blue), HEM (orange) and

IMR (red) is shown in Fig. 5 and corresponding error PDFs for six homogeneous monsoon regions are in Fig. 6. All the SPPs are following IMD rainfall (gradual increasing rainfall from June to August and decreasing from August to September) in estimating the daily rainfall with different magnitudes (Fig. 5 a – f). GPM captures the seasonal mean rainfall reasonably as compared to other satellite products. GPM is shown to have a closer relationship with IMD in six homogeneous regions than other products. GPM over all the regions has been shown comparatively less error (about zero) at high frequency over most of the sub-regions (Fig. 6 a – f).

The grid-to-grid errors obtained from the GPM are low RMSE and bias, and high correlation values (shown in Fig. 7) over all regions. Such better performance could be attributed to the procedure involved in developing of GPM products, as discussed above. The rainfall estimations from TRMM, HEM, and IMR show overestimation on a daily scale over all regions of India. TRMM, HEM, and IMR have shown less frequency for less rainfall error (as shown in Fig. 5) and a higher bias, RMSE and reasonable correlation values (shown in Fig. 7). The reason for overestimation is that TRMM, HEM and IMR rainfall algorithm mainly uses TIR channel rainfall information which computes the cloud top brightness temperature (CTBT) (Gairola et al. 2015). The CTBT is more in all homogeneous regions because

the Arabian Sea and Bay of Bengal branches bring more moisture towards India, resulting in the formation of clouds (Gadgil and Kumar 2006). On the other hand, the HEM is carried out with several corrections such as orographic correction and atmospheric correction (Kumar and Varma 2017) which results in the HEM into a better analysis compared with IMR in estimating the ISMR.

Figure 8 represents the frequency distribution of monthly (JJAS) rainfall for light, moderate and heavy rainfall categories over different homogenous regions of India. Here, GPM is performing well over all sub-regions in estimating the light, moderate categories than other products in all months and followed by TRMM, HEM and IMR. For heavy rainfall, HEM and IMR have been completely overestimated. Among the four satellite products, GPM is showing close agreement in estimating JJAS rainfall with IMD for all rainfall thresholds over all regions of India. Furthermore, the performance of satellite products for light, moderate and heavy rainfall thresholds have been estimated in terms of POD, FAR, and ETS for the season. The averaged skill scores are discussed in Fig. 9. It is noticed that for the light rainfall category, GPM is showing reasonably good agreement over all regions (with a high POD (80%), low FAR (10%), and higher ETS (0.75) as compared to others except over the NE region (with a poor POD (40%), higher FAR and less ETS). A recent study by Prakash et al. (2018) pointed out that the

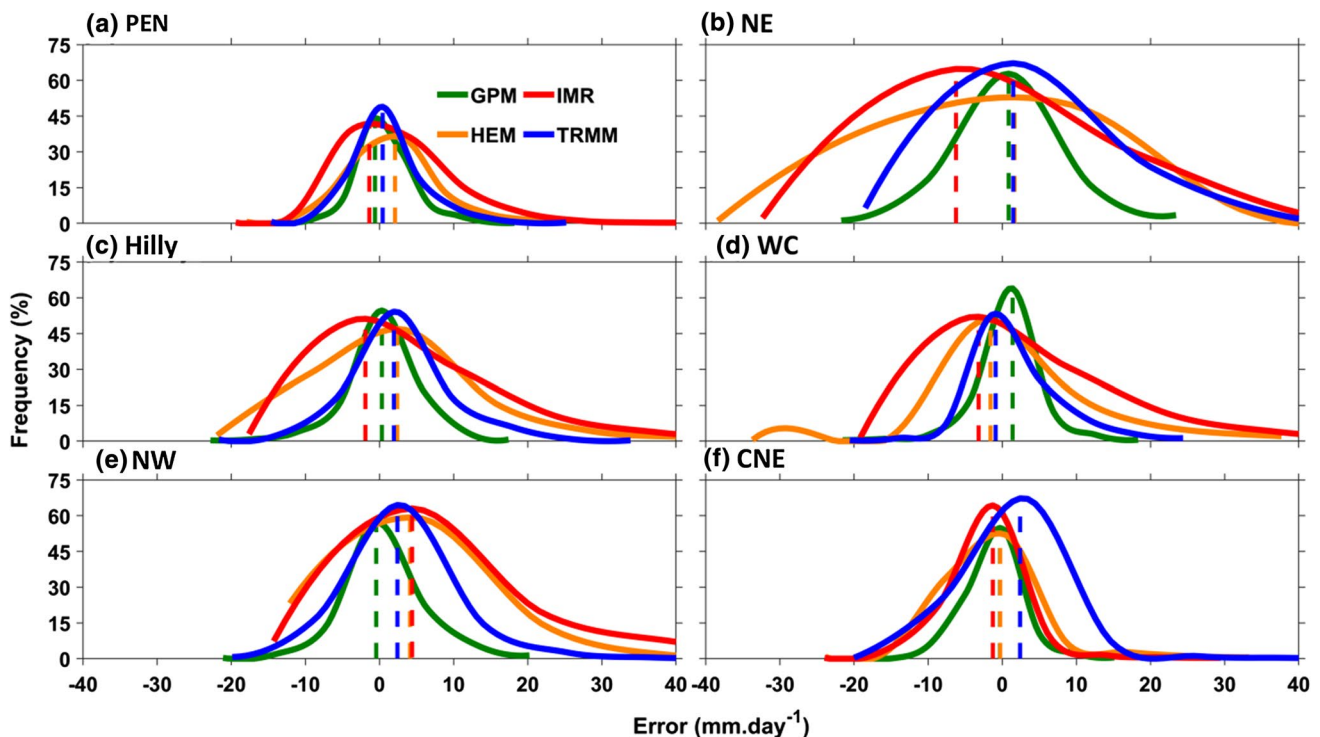
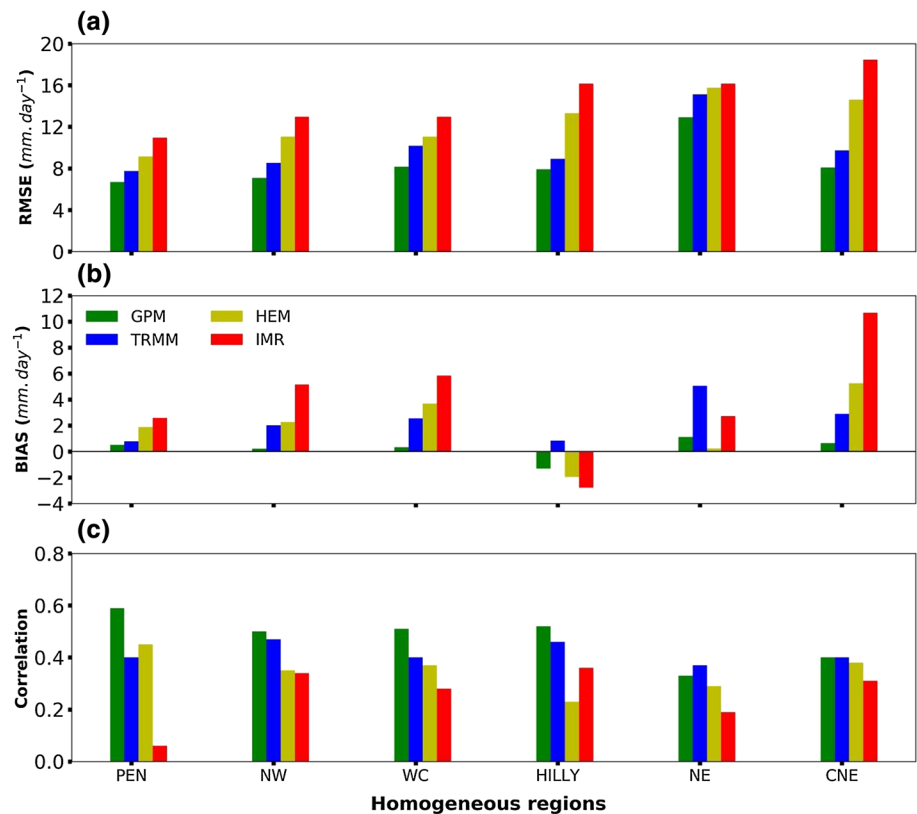


Fig. 6 Error PDFs of seasonal rainfall of GPM, TRMM, HEM and IMR over six homogeneous regions **a** PEN, **b** NE, **c** Hilly, **d** WC, **e** NW, **f** CNE. The error is calculated against IMD rainfall

Fig. 7 Grid-wise errors of satellite products (GPM, TRMM, HEM and IMR) over different homogeneous regions **a** RMSE (mm day^{-1}) **b** bias (mm day^{-1}), and **c** correlation coefficient



SPPs (GPM, and TRMM) are facing difficulties in the rain detection process over the PEN and NE regions of India. The HEM showed better categorical verification statistics over the NE region and could be due to orographic and atmospheric corrections in rainfall estimation (Prakash et al. 2015b, c, a). In the case of moderate rainfall, both GPM and TRMM estimates can capture the satellite estimated values with slight variations between them. For instance, NE, Hilly, and WC regions show higher POD values in the TRMM product. Contrastingly, FAR shows the lower values for the GPM product. It infers that both the GPM and TRMM detect the rainfall events in more or less uniform. Considering the heavy rainfall, GPM, TRMM, HEM and IMR products are unable to predict the rainfall events in all homogeneous regions. For example, TRMM and IMR products are unable to capture the rainfall occurrence over the PEN and CNE regions (Fig. 9). It is further noticed that for the higher rainfall category, all the remaining satellite products also showed poor performance when compared to each other.

4.3 Evaluation of rainfall products in extreme monsoon years

In addition, the present analysis is extended to check the reliability of satellite products in estimating the summer seasonal rainfall during deficit and normal years. According to IMD, 2015 and 2016 are deficit and normal years and

received the monsoonal rainfall of about 86.4 and 97%. Figure 10a–h shows the statistical analysis of JJAS rainfall during 2015–2016. Among all the satellite products, the GPM performs better in both deficit (2015) and normal (2016) monsoon years with lower RMSE (18.4 mm day^{-1} and 19.4 mm day^{-1} respectively). The TRMM rainfall exhibits higher RMSE ($> 22 \text{ mm day}^{-1}$) for both deficit and normal years, slightly higher than the GPM. The IMR performs better for deficit years with less RMSE (20.7 mm day^{-1}), which is higher (37.5 mm day^{-1}) for a normal year (Fig. 10d). The HEM has resulted in higher errors, unlike the other products. Comparison of bias among the products, the GPM shows the least bias of $+0.6 \text{ mm day}^{-1}$ and $+0.2 \text{ mm day}^{-1}$, respectively, for the deficit and normal years (Fig. 10a, e). The IMR rainfall is highly biased (10.4 mm day^{-1}) to show excess rainfall in a normal year compared to the others (Fig. 10h). The PDFs suggest that rainfall events of 12 mm day^{-1} are frequent (10%) in deficit year (Fig. 10i), while $8\text{--}10 \text{ mm day}^{-1}$ is common at 12% in the normal year (Fig. 10j) as revealed from IMD. Similar rainfall occurrence (about 10 mm day^{-1}) is seen in GPM product at a similar frequency in deficit year and slightly higher frequency in a normal year. In contrast, the TRMM rainfall indicates higher rainfall activity ($14\text{--}15 \text{ mm day}^{-1}$) with 7–10% frequency in both deficit and normal years (Fig. 10i, j). HEM shows similar rainfall activity as seen in the IMD with less frequency. In the case of IMR, the rainfall PDF in the deficit

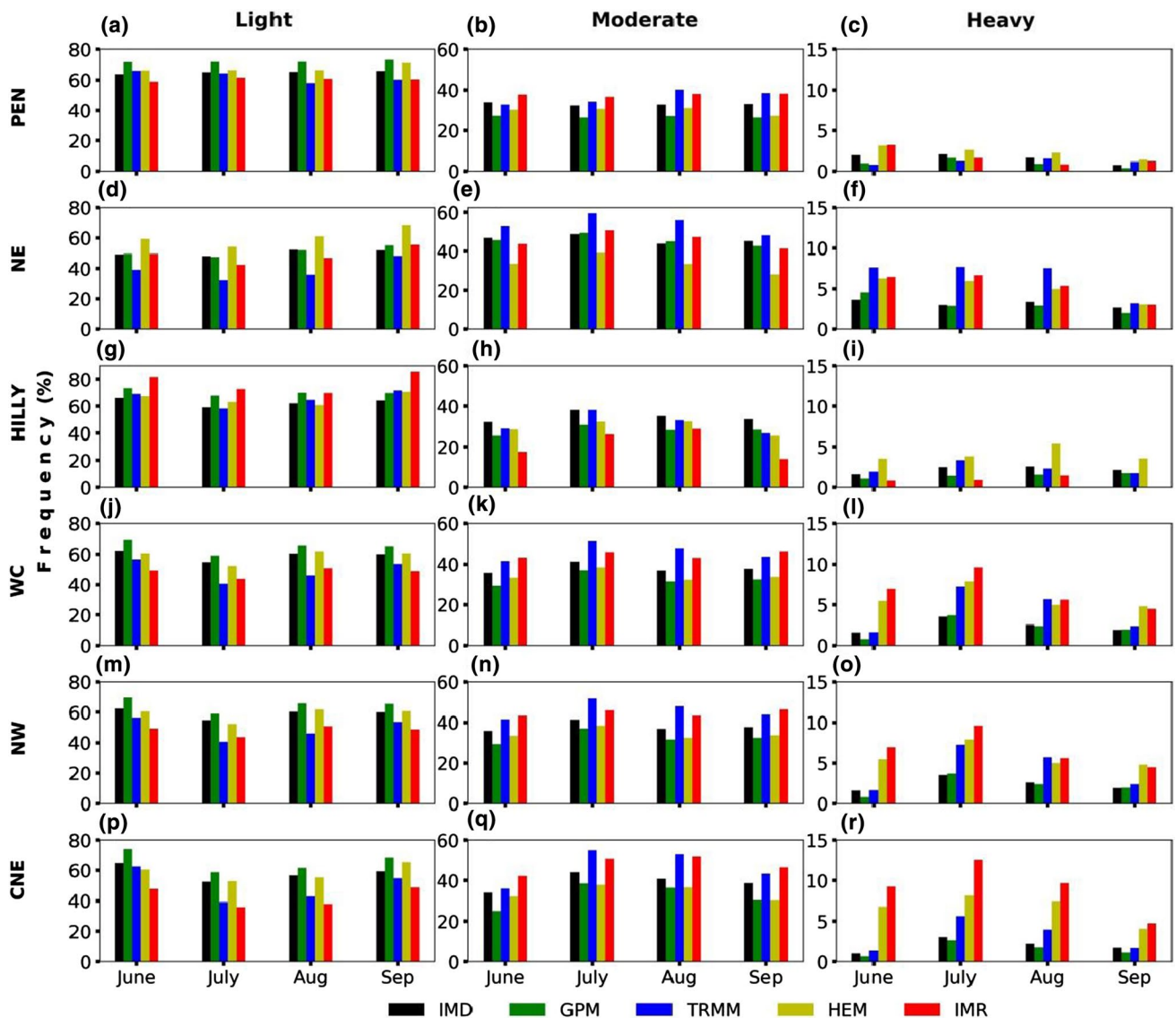


Fig. 8 Frequency distribution (%) of area averaged monthly rainfall over homogeneous regions for **a** light rainfall **b** moderate and **c** heavy rainfall over Peninsular India (PEN). **d–f**, **g–i**, **h–l**, **m–o**, and **p–r** are same as **a–c** but for NE, Hilly, WC, NW, and CNE regions, respectively

year is relatively better than the normal year. In the normal year, the IMR shows higher rainfall activity (20 mm day^{-1}) at less frequency.

The spatial distribution of seasonal mean rainfall for light and moderate categories for the deficit and normal years are presented in Fig. 11. Note that there is no heavy rainfall ($> 64.5 \text{ mm day}^{-1}$) during these both deficit and normal years. The pattern correlation for light rainfall threshold in normal (deficit) year obtained from the GPM, TRMM, HEM and IMR are 0.85 (0.71), 0.71 (0.54), 0.66 (0.45), and 0.60 (0.39), respectively, over India. Similarly, for moderate rainfall 0.71 (0.58), 0.30 (0.43), 0.15 (0.28), -0.34 (0.14). The spatial patterns of light rainfall are well captured in GPM for deficit (Fig. 11a–e) and normal (Fig. 11f–j) years. While

the TRMM, HEM, and IMR appear to be better in replicating the patterns over northwest and southern parts of India but are poor over Gangetic plains of India in deficit year. The representation of light rain in a normal year by these products is poorer than that in a deficit year. The moderate rainfall is mainly confined to the west coast, central and northeast parts of India as revealed in the IMD rainfall in deficit and normal years (Fig. 11k, p). Similar spatial patterns are realistically drawn in GPM rainfall in both deficit and normal years, followed by the TRMM rainfall. Comparing INSAT-3D rainfall products, the HEM appears better than IMR in representing moderate rainfall for the deficit and normal years. IMR overestimates the observed rainfall noticeably.

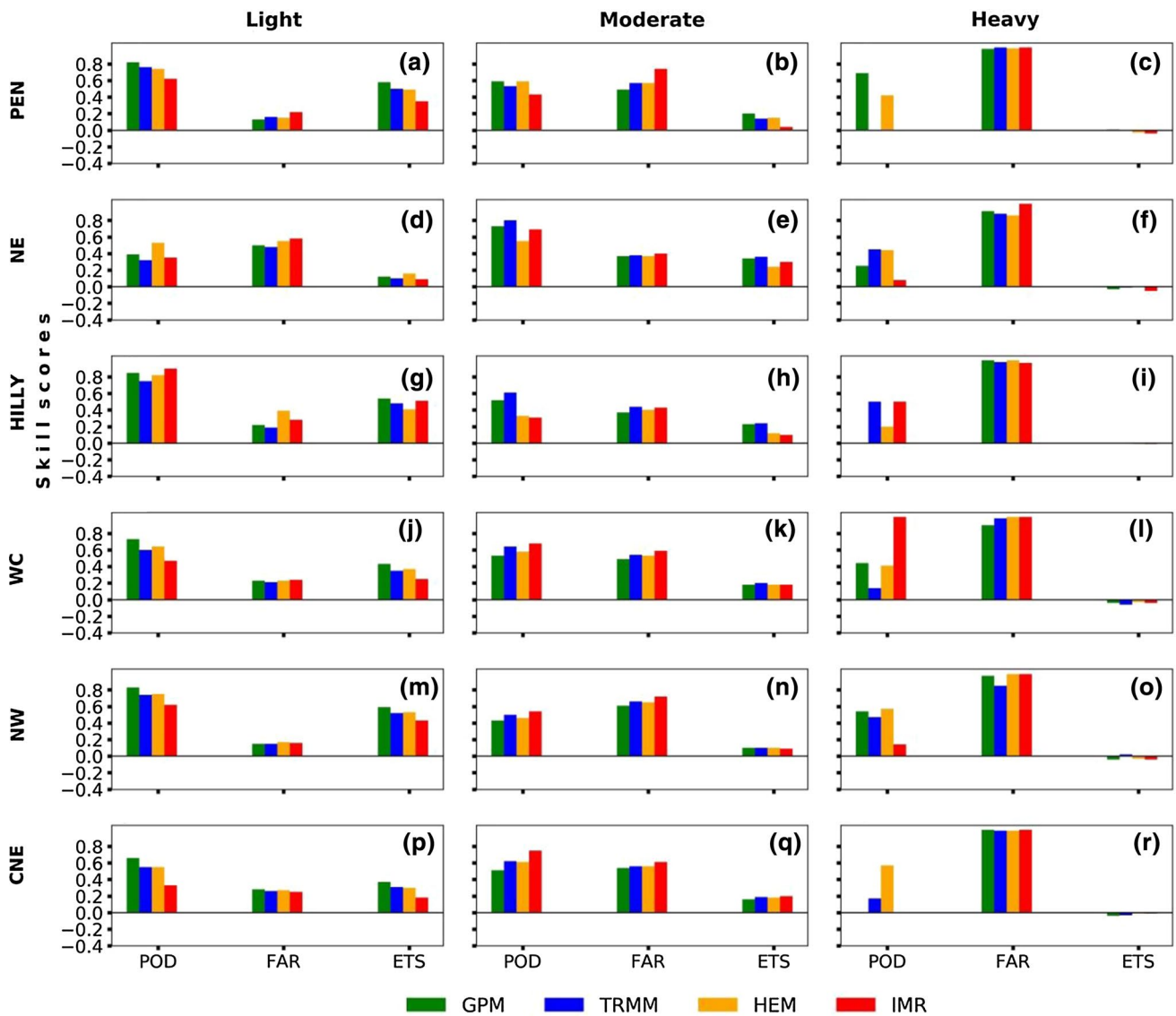


Fig. 9 Skill scores (POD, FAR and ETS) of area averaged seasonal rainfall (mm day⁻¹) over homogeneous regions for **a** light rainfall **b** moderate and **c** heavy rainfall over Peninsular India (PEN). **d–f**, **g–i**,

h–l, **m–o**, and **p–r** are same as **a–c** but for NE, Hilly, WC, NW, and CNE regions, respectively

4.4 Evaluation of satellite rainfall products for daily extreme rainfall activity

Monsoon is known to produce heavy to very heavy rainfall across the various temporal scales starting from daily to seasonal. The daily extreme rainfall activity causes loss of lives and property due to flash floods, landslides, etc. Therefore, the value of the satellite products has been evaluated in representing the daily extreme rainfall events. Goswami et al (2006) demonstrated that the rainfall (RF) in central India (75.30°E–86.63°E, 16.92°N–26.43°N) represents all India average rainfall during summer monsoon. Therefore, this region is considered for this analysis. For this, we have

divided the rainfall activities as lowest rain, normal rain and highest rains in central India based on standard deviation (std) values. The rainfall extremes vary from place to place within the season. Hence, the rainfall extremes are defined as follows.

Lowest rain activity: $\text{rainfall} < \text{RF}_{\text{mean}} - \text{RF}_{\text{std}}$
 Normal rain Activity : $\text{RF}_{\text{mean}} - \text{RF}_{\text{std}} < \text{Rainfall} < \text{RF}_{\text{mean}} + \text{RF}_{\text{std}}$
 Highest rain Activity: $\text{rainfall} > \text{RF}_{\text{mean}} + \text{RF}_{\text{std}}$

RF_{mean} and RF_{std} have represented the mean and standard deviation of rainfall. Figure 12 shows the cumulative distribution function (CDF) of daily rainfall for (a) lowest rain (b) normal rain, and (c) highest rain from the satellite

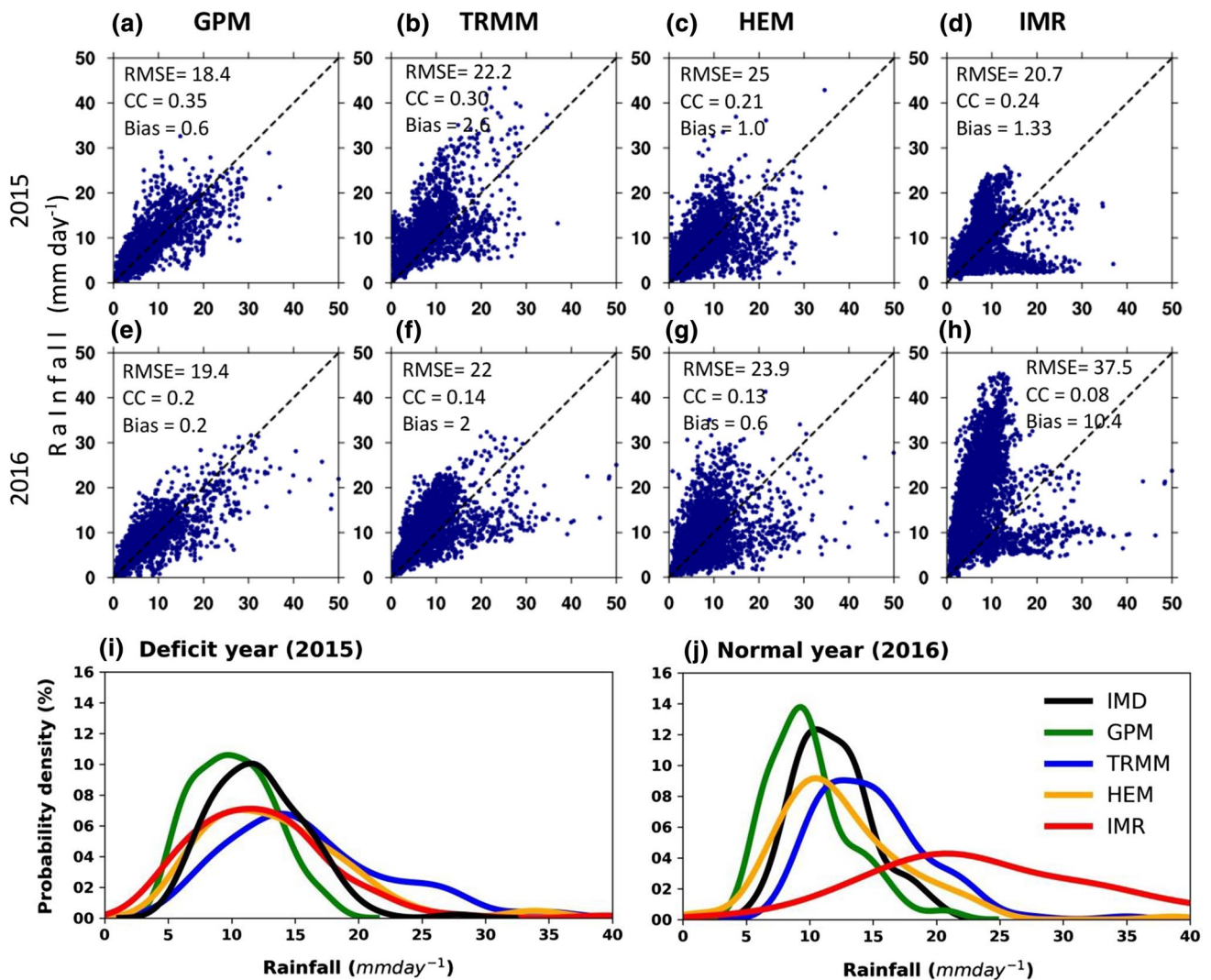


Fig. 10 Verification of area averaged daily JJAS rainfall from **a** GPM, **b** TRMM, **c** HEM, and **d** IMR products against IMD rainfall for deficit year (2015) and normal year (2016). Respective RMSE and cor-

relation are given in each plot. PDF (%) of rainfall occurrence from GPM, TRMM, HEM and IMR products are for **i** deficit year and **j** normal year

precipitation products (GPM, TRMM, HEM, and IMR) along with the IMD observation from 2014 to 2019. As observed from IMD, the mean daily rainfall over central India during the monsoon season is ~ 7.1 mm, with a standard deviation of ~ 5.2 mm. As seen in the earlier analysis, the GPM could capture the mean rainfall and its variation (7.4 and 5.6 mm) as observed. The remaining products show higher magnitudes in terms of mean and standard deviation. For instance, the TRMM-derived mean rainfall is 8.8 mm and the standard deviation is 6.8 mm. Similarly, the IMR and HEM could show much higher mean rainfall activity (21.5 and 12 mm) and standard deviation (18 and 10.3 mm, respectively).

The CDF indicates that the lowest rains daily lie within 5 mm in the IMD observations. Though the GPM slightly underestimates the same, it follows the IMD pattern with

good agreement. The TRMM and IMR overestimate (up to 8.5–10 mm) the lowest rains for any CDF value when compared with IMD. The HEM appears to be better for the rainfall up to 2.5 mm after which it overestimates the lowest rains (Fig. 12a). Considering normal rainfall, both GPM and TRMM replicate the observed (IMD) rainfall pattern confining to the rainfall activity of 7–27 mm, while the IMR and HEM highly overestimate the normal daily rainfall (Fig. 12b). Similarly, the GPM and TRMM perform better in capturing the highest rains in a day. There is a noticeable difference between the IMR/HEM and IMD CDFs, indicating an overestimation of the INSAT-derived rainfall products (Fig. 12c). Overall analysis demonstrates that the GPM can capture all categories of daily rainfall activity compared with other satellite rainfall products. Higher standard deviations in the case of INSAT-rainfall products indicate its capability

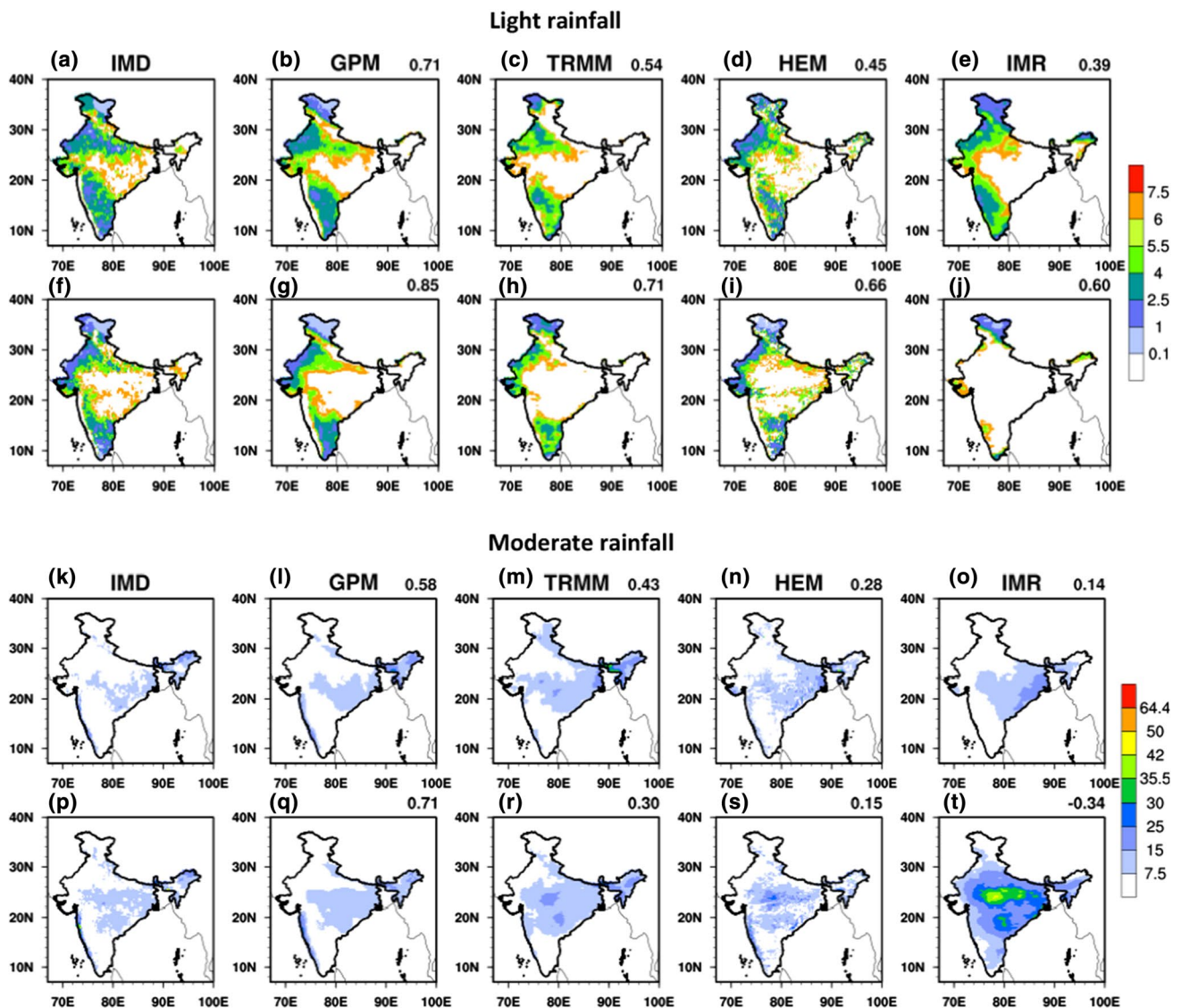


Fig. 11 Spatial distribution of light rainfall category during summer monsoon from **a** GPM **b** TRMM **c** HEM and **d** IMR for deficit year (2015). **e–h** are same as **a–d** but for normal year (2016). **i–j** and **k–n** are the same as **a–d** and **e–h** but for moderate rainfall

to capture maximum extremes of daily rainfall compared to GPM and TRMM.

5 Summary and conclusions

Satellite-derived rainfall products have been useful and act as an alternative tool for understanding the monsoon rainfall characteristics (Intra-seasonal oscillations) and evaluating the model rainfall products. The present study assesses the advantage of using high-resolution satellite rainfall products over the Indian regions.

In this study, four satellite-derived rainfall products namely, GPM, IMR, HEM, and TRMM were evaluated against IMD rainfall during 2014–2019. The evaluation is

carried out at daily, monthly and seasonal scales over different homogeneous rainfall regions. The GPM product has shown good performance in capturing the mean spatial features such as orographic rainfall over India on a seasonal scale, with less bias (0.25), RMSE (7.2) and a higher correlation coefficient (0.73) as compared to the other satellite products. The GPM has reasonably captured All-India rainfall at daily, monthly, and seasonal scales than the others. Furthermore, categorical skill scores such as POD, FAR, and ETS reveals that GPM can identify light and moderate rainfall better with a high POD (80%), less FAR (10%), and high ETS (75%) than the other satellite products. The heavy rainfall ($> 64.5 \text{ mm day}^{-1}$) is not captured well in all the satellite products.

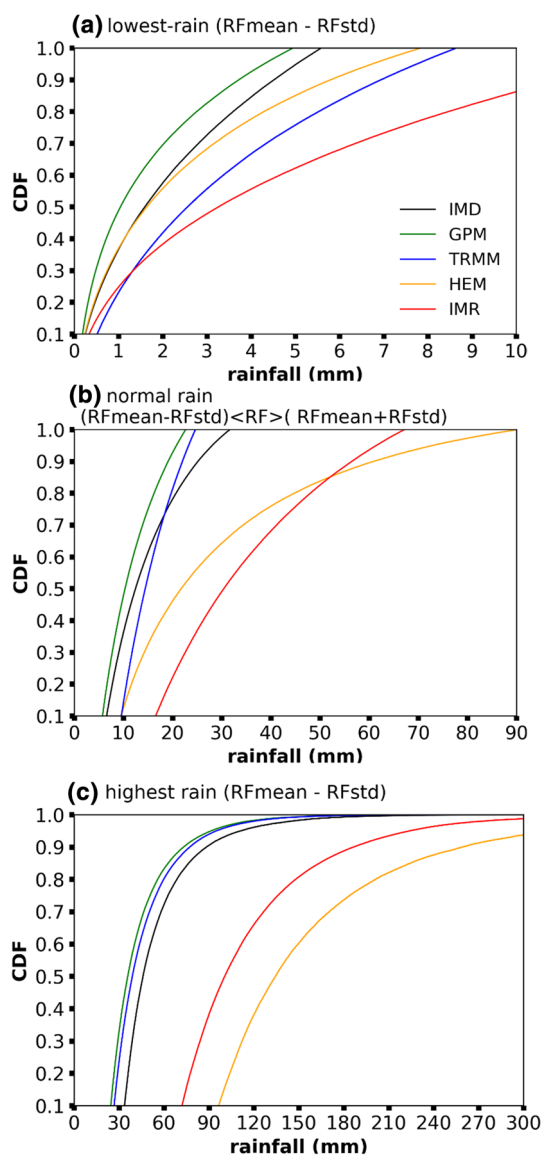


Fig. 12 The cumulative distribution function (CDF) of daily rainfall over central India for **a** lowest rain, **b** normal rain, and **c** highest rain from GPM, TRMM, HEM, and IMR products along with the IMD observation. X-axis indicates the rainfall in mm

The evaluation of satellite rainfall over six homogeneous regions (PEN, NE, Hilly, WC, NW, CNE) of India reveals that the GPM has shown reasonable accuracy (high CC, lower bias and RMSE) over all homogeneous regions when compared with IMD. Considering categorical skill scores over all regions, the GPM performs well for light and moderate rainfalls with high POD, less FAR and high ETS than other satellite products. In case of heavy rainfall, all the satellite products have shown poor skill scores, however, the GPM is comparatively better.

The rainfall products are also evaluated for extreme monsoon years and realized that the rainfall in deficit and normal

years is better represented by the GPM than TRMM, HEM, and IMR. The PDF of rainfall occurrences also indicates better GPM rainfall performance (10–14%) with that of IMD (9–12%) in extreme years. IMR shows poor performance for a normal year, whereas for deficit year, IMR and HEM perform well with rainfall underestimation. The analysis of the extremes also indicating that GPM is performing better estimator and followed by TRMM. The HEM and IMR products could capture extremely heavy rainfall, because of their higher standard deviation values. Overall results reveal that the GPM can show the spatial and temporal structures of rainfall followed by TRMM, HEM and IMR. Note that the accuracy may vary when considering the long-term dataset in the verification. It is envisaged that the performance of HEM and IMR products may be improved by merging with rain-gauge data, adopting suitable bias correction and introducing hydrometeors information.

Acknowledgements The authors duly acknowledge the financial support of Earth System Science Organization (ESSO), Ministry of Earth Sciences (MoES/16/14/2014-RDEAS). The computational facility acquired through the grant of Scientific Engineering Research Board (SERB) Grant (ECR/2016/001637), Govt. of India is acknowledged.

Data availability and materials The data that support the findings of this study are available from the corresponding author upon request.

Declarations

Conflicts of interest The authors declare that they have no known competing interests for this publication.

References

- Ankur K, Busireddy NKR, Osuri KK, Niyogi D (2020) On the relationship between intensity changes and rainfall distribution in tropical cyclones over the North Indian Ocean. *Int J Climatol* 40(4):2015–2025
- Ba M, Gruber A (2001) GOES multispectral rainfall algorithm (GMSRA). *J Appl Meteorol* 40(8):1500–1514
- Barrett EC and Martin DW (1981) The use of satellite data in rainfall monitoring, Academic Press (London), pp. xii+ 340.
- Bushair MT, Kumar P, Gairola RM (2019) Evaluation and assimilation of various satellite-derived rainfall products over India. *Int J Remote Sens* 40(14):5315–5338
- Derin Y, Yilmaz KK (2014) Evaluation of multiple satellite-based precipitation products over complex topography. *J Hydrometeorol* 15(4):1498–1516. <https://doi.org/10.1175/jhm-d-13-0191.1>
- Dinku T, Chidzambwa S, Ceccato P, Connor SJ, Ropelewski CF (2008) Validation of high-resolution satellite rainfall products over complex terrain. *Int J Remote Sens* 29(14):4097–4110. <https://doi.org/10.1080/01431160701772526>
- Gadgil S (1977) Orographic effects on the southwest monsoon: a review. *Pure Appl Geophys* 115(5–6):1413–1430. https://doi.org/10.1007/978-3-0348-5759-8_16
- Gadgil S, Kumar KR (2006) The Asian monsoon agriculture and economy. *The Asian monsoon*. Springer, Berlin, Heidelberg, pp 651–683

- Gairola RM, Prakash S, Bushair MT, Pal PK (2014) Rainfall estimation from Kalpana-1 satellite data over Indian land and oceanic regions. *Curr Sci* 1275-1282
- Gairola RM, Prakash S, Pal PK (2015) Improved rainfall estimation over the Indian monsoon region by synergistic use of Kalpana-1 and rain gauge data. *Atmosfera* 28(1):51–61
- Goswami BN et al (2006) Increasing trend of extreme rain events over India in a warming environment. *Sci* 314(5804):1442–1445
- Guhathakurta P, Rajeevan M (2008) Trends in the rainfall pattern over India. *Int J Climatol* 28(11):1453–1469
- Houze RA Jr (2012) Orographic effects on precipitating clouds. *Rev Geophys.* <https://doi.org/10.1029/2011rg000365>
- Huffman GJ, Bolvin DT, Braithwaite D, Hsu K, Joyce R, Xie P (2015) NASA Global Precipitation Measurement Integrated Multi-satellite Retrievals for GPM (IMERG). http://pmm.nasa.gov/sites/default/files/document_files/IMERG_ATBD_V4.5.pdf. Accessed on 12 September 2016.
- Huffman GJ, Bolvin DT, Nelkin EJ, Stocker EF, Tan J (2017) V04 IMERG Final Run Release Notes NASA Goddard Earth Sciences Data and Information Services Center: Greenbelt, MD, USA. https://pmm.nasa.gov/sites/default/files/document_files/IMERG_QI.pdf Accessed on 21 March 2017
- Huffman GJ, Bolvin DT, Braithwaite D, Hsu K, Joyce R, Xie P, Yoo SH. NASA global precipitation measurement (GPM) integrated multi-satellite retrievals for GPM (IMERG). Algorithm Theoretical Basis Document (ATBD) Version 06. https://gpm.nasa.gov/sites/default/files/2020-05/IMERG_ATBD_V06.3.pdf. Accessed on 3 January 2020
- Huffman GJ, Bolvin DT, Nelkin EJ, Wolff DB, Adler RF, Gu G, Hong Y, Stocker EF, Bowman KP (2007) The TRMM multisatellite precipitation analysis (TMPA): Quasi-global, multiyear, combined-sensor precipitation estimates at fine scales. *J Hydrometeorol* 8(1):38–55
- Jiang S, Ren L, Hong Y, Yong B, Yang X, Yuan F, Ma M (2012) Comprehensive evaluation of multi-satellite precipitation products with a dense rain gauge network and optimally merging their simulated hydrological flows using the Bayesian model averaging method. *J Hydrol* 452:213–225
- Krishnamurthy V, Kinter JL (2003) The Indian monsoon and its relation to global climate variability. *global climate*. Springer, Berlin, Heidelberg, pp 186–236
- Krishnamurthy V, Shukla J (2007) Intraseasonal and seasonally persisting patterns of Indian monsoon rainfall. *J Clim* 20(1):3–20
- Kumar P, Varma AK (2017) Assimilation of INSAT-3D hydro-estimator method retrieved rainfall for short-range weather prediction. *Q J R Meteorol Soc* 143(702):384–394
- Kumar TVL, Barbosa HA, Thakur MK, Paredes-Trejo F (2019) Validation of satellite (TMPA and IMERG) rainfall products with the IMD gridded data sets over monsoon core region of India In *Satellite Information Classification and Interpretation*. IntechOpen. Rustam B. Rustamov (Ed), pp 105–116. <https://doi.org/10.5772/intechopen.77202>
- Kummerow C, Barnes W, Kozu T, Shiue J, Simpson J (1998) The tropical rainfall measuring mission (TRMM) sensor package. *J Atmos Oceanic Technol* 15(3):809–817. [https://doi.org/10.1175/1520-0426\(1998\)015%3c0809:TTRMMT%3e2.0.CO;2](https://doi.org/10.1175/1520-0426(1998)015%3c0809:TTRMMT%3e2.0.CO;2)
- Larson LW, Peck EL (1974) Accuracy of precipitation measurements for hydrologic modeling. *Water Resour Res* 10(4):857–863
- Liu X, Yang T, Hsu K, Liu C, Sorooshian S (2017) Evaluating the streamflow simulation capability of PERSIANN-CDR daily rainfall products in two river basins on the Tibetan Plateau. *Hydrol Earth Sys Sci* 21(1):169–181
- Lakshmi Kumar TV, Rao KK, Uma R, Aruna K (2014) The role of El Niño Southern Oscillation on the patterns of cycling rates observed over India during the monsoon season. *J Water Climate Change* 5(4):696–706
- Mei Y, Anagnostou EN, Nikolopoulos EI, Borga M (2014) Error analysis of satellite precipitation products in mountainous basins. *J Hydrometeorol* 15(5):1778–1793
- Mitra AK, Bohra AK, Rajeevan MN, Krishnamurti TN (2009) Daily Indian precipitation analysis formed from a merge of rain-gauge data with the TRMM TMPA satellite-derived rainfall estimates. *J Meteorol Soc Jpn* 87:265–279
- Mitra AK, Momin IM, Rajagopal EN, Basu S, Rajeevan MN, Krishnamurti TN (2013) Gridded daily Indian monsoon rainfall for 14 seasons: Merged TRMM and IMD gauge analyzed values. *J Earth Sys Sci* 122(5):1173–1182
- Mitra AK, Kaushik N, Singh AK, Parihar S, Bhan SC (2018) Evaluation of INSAT-3D satellite derived precipitation estimates for heavy rainfall events and its validation with gridded GPM (IMERG) rainfall dataset over the Indian region. *Remote Sens Appl: Soc Environ* 9:91–99
- Mukhopadhyay P, Prasad VS, Krishna RPM, Deshpande M, Ganai M, Tirkey S, Rajeevan M (2019) Performance of a very high-resolution global forecast system model (GFS T1534) at 12.5 km over the Indian region during the 2016–2017 monsoon seasons. *J Earth Syst Sci* 128(6):1–18
- Nair S, Srinivasan G, Nemani R (2009) Evaluation of multi-satellite TRMM derived rainfall estimates over a western state of India. *J Meteorol Soc Jpn Ser II* 87(6):927–939
- Osuri KK, Ankur K, Nadimpalli R, Busireddy NK (2020) Error characterization of ARW model in Forecasting tropical cyclone rainfall over North Indian Ocean. *J Hydrol* 590:125433. <https://doi.org/10.1016/j.jhydrol.2020.125433>
- Pai DS, Sridhar L, Rajeevan M, Sreejith OP, Satbhai NS, Mukhopadhyay B (2014) Development of a new high spatial resolution (0.25° × 0.25°) long period (1901–2010) daily gridded rainfall data set over India and its comparison with existing data sets over the region. *Mausam* 65(1):1–18. <https://doi.org/10.1007/s00382-014-2307-1>
- Pai DS, Sridhar L, Rajeevan M et al (2015) Analysis of the daily rainfall events over India using a new long period (1901–2010) high resolution (0.25° × 0.25°) gridded rainfall data set. *Clim Dyn* 45:755–776. <https://doi.org/10.1007/s00382-014-2307-1>
- Parthasarathy B, Munot AA, Kothawale DR (1995) Monthly and seasonal rainfall series for all-India homogeneous regions and meteorological subdivisions: 1871–1994. IITM research report No. RR-065, available from Indian Institute of Tropical Meteorology, Pashan, Pune-411 008, India
- Prakash S, Sathiyamoorthy V, Mahesh C, Gairola RM (2014) An evaluation of high-resolution multisatellite rainfall products over the Indian monsoon region. *Int J Remote Sens* 35(9):3018–3035
- Prakash S, Mitra AK, AghaKouchak A, Pai DS (2015a) Error characterization of TRMM multisatellite precipitation analysis (TMPA-3B42) products over India for different seasons. *J Hydrol* 529:1302–1312. <https://doi.org/10.1016/j.jhydrol.2015.08.062>
- Prakash S, Mitra AK, Momin IM, Pai DS, Rajagopal EN, Basu S (2015b) Comparison of TMPA-3B42 versions 6 and 7 precipitation products with gauge-based data over India for the southwest monsoon period. *J Hydrometeorol* 16(1):346–362
- Prakash S, Mitra AK, Pai DS (2015c) Comparing two high-resolution gauge-adjusted multisatellite rainfall products over India for the southwest monsoon period. *Meteorol Appl* 22(3):679–688
- Prakash S, Mitra AK, AghaKouchak A, Liu Z, Norouzi H, Pai DS (2018) A preliminary assessment of GPM-based multi-satellite precipitation estimates over a monsoon dominated region. *J Hydrol* 556:865–876
- Rahman SH, Sengupta D, Ravichandran, M (2009) Variability of Indian summer monsoon rainfall in daily data from gauge and satellite. *J Geophys Res Atmos* 114(D17).

- Rajeevan M et al (2006) High resolution daily gridded rainfall data for the Indian region: analysis of break and active monsoon spells. *Curr Sci* 91(3):296–306
- Reddy MV, Mitra AK, Momin IM, Mitra AK, Pai DS (2019) Evaluation and inter-comparison of high-resolution multi-satellite rainfall products over India for the southwest monsoon period. *Int J Remote Sens* 40(12):4577–4603
- Shepard, and Donald (1968) A two-dimensional interpolation function for irregularly-spaced data. Proceedings of the 1968 23rd ACM national conference.
- Singh AK, Singh V, Singh KK, Tripathi JN, Kumar A, Sateesh M, Peshin SK (2018) Validation of INSAT-3D derived rainfall estimates (HE & IMSRA), GPM (IMERG) and GLDAS 21 model rainfall product with IMD gridded rainfall & NMSG data over IMD's meteorological sub-divisions during monsoon. *Mausam* 69(2):177–192
- Sun Q, Miao C, Duan Q, Ashouri H, Sorooshian S, Hsu KL (2018) A review of global precipitation data sets: data sources, estimation, and inter comparisons. *Rev Geophys* 56(1):79–107
- Thakur MK, Kumar TL, Narayanan MS, Kundeti KR, Barbosa H (2020) Analytical study of the performance of the IMERG over the Indian landmass. *Meteorol Appl* 27(3):1908
- Tapiador FJ, Turk FJ, Petersen W, Hou AY, García-Ortega E, Machado LA, Angelis CF, Salio P, Kidd C, Huffman GJ, De Castro M (2012) Global precipitation measurement: Methods, datasets and Applications. *Atmos Res* 104:70–97. <https://doi.org/10.1016/j.atmosres.2011.10.021>
- Turner AG, Annamalai H (2012) Climate change and the South Asian summer monsoon. *Nat Clim Change* 2(8):587–595
- Uma R, Kumar TL, Narayanan MS, Rajeevan M, Bhate J, Kumar KN (2013) Large scale features and assessment of spatial scale correspondence between TMPA and IMD rainfall datasets over Indian landmass. *J Earth Sys Sci* 122(3):573–588
- Vicente G, Scofield A, Menzel P (1998) The operational GOES infrared rainfall estimation technique *Bull. Am Meteorol Soc* 79(9):1883–1898

Publisher's Note Springer Nature remains neutral with regard to jurisdictional claims in published maps and institutional affiliations.